Ionosphere Scintillation Modelling / Satellite Navigation Impairments & Radar Observations

Y. Béniguel, P. Hamel
IEEA
Courbevoie, France
beniguel@ieea.fr

Abstract— **The formulation of a wave propagation model through a turbulent ionosphere is presented. The calculation of the transmitted field enables the estimation of signal impairments, especially its intensity and phase fluctuations. The model outputs are compared with measurement results. This was performed for the intensity and phase fluctuation levels and for the spectral content of the transmitted signal. The field second order moment calculation is then presented. The Mutual Coherence Function characterizes the channel transfer function. It is required for radar performances assessment after propagation through the turbulent medium. It was demonstrated that under simplified hypothesis, an analytical solution can be derived allowing a sensitivity analysis study.**

Keywords-scintillation, ionosphere, parabolique equetion

I. INTRODUCTION

The signal fluctuations, referred as scintillations, are created by random fluctuations of the medium's refractive index, which are caused by inhomogeneities inside the ionosphere. These inhomogeneities are sub structures of bubbles, which may reach dimensions of several hundreds of kilometers as can be seen from radar observations (Costa et al, 2011). These bubbles present a patchy structure. They appear after sunset, when the sun ionization drops to zero. Instability processes develop inside these bubbles with creation of turbulences inside the medium. As a result, depletions of electron density appear. In the L band and for the distances usually considered, the diffracting pattern of inhomogeneities in the range of one kilometer size, is inside the first Fresnel zone and contribute to scintillation.

Ionosphere scintillation is currently the object of many measurement campaigns, both at low and high latitudes. The main campaigns related to the areas covered by experimentation are the Low Latitude Ionospheric Sensor network (LISN) in South America (Valladares, 2009), the SCINDA network in America and Africa (Carrano, 2006) and the CHAIN network in Canada (Jayachandran, 2009). But there are many others worldwide. In this paper, we will refer to the PRIS measurement campaign conducted in the frame of an ESA / ESTEC contract during years 2005 – 2006, with measurements at low and high latitudes (Béniguel, 2009).

This study was supported by ESA / ESTEC

A propagation model aiming at reproducing the signal fluctuations is presented in this paper. The calculation addresses the evaluation of the transmitted field and of its second order moment. In most cases, as in GNSS applications, the knowledge of the transmitted field allows estimating the degradation of performances, due to both intensity and phase fluctuations. The paper presents some comparisons of intensity scintillation modeling with measurements. For radar observations, the knowledge of the second order moment is also required. The signal coherence properties of the medium, both for time and frequency, are important in this case to assess the radar performances. One example is presented including the radar antenna pattern in the case of a SAR antenna.

II. SCATTERED FIELD CALCULATION

A. Introduction

The model presented in this paper (Global Ionospheric Scintillation Propagation Model (GISM)) uses the Multiple Phase Screen technique (MPS) (Knepp, 1983, Béniguel, 2011, Gherm, 2005). The locations of transmitter and receiver are arbitrary. The incidence link angle is arbitrary regarding the ionosphere layers and to the magnetic field vector orientation. It can cross the entire ionosphere or a small part of it. At each screen location along the line of sight, the parabolic equation (PE) is solved. GISM allows calculating mean errors and scintillations due to propagation through the ionosphere.

The mean errors are obtained using a ray technique solving the Haselgrove equations. The ionosphere electronic density at any point inside the medium, required for this calculation, is provided by the NeQuick model (Radicella, 2009), which is included in the GISM.

The line of sight being determined, the fluctuations are calculated in a second stage using the multiple phase screen technique. The medium is divided into successive layers, each of them acting as a phase screen. In this technique, which is detailed hereafter, the field is scattered from one screen to the next one.

B. Theoretical Formulation

The wave propagation is calculated solving the Helmholtz equation (Ishimaru, 1978).

$$\left[\nabla^2 + k^2 \left(1 + \varepsilon_1(\bar{r})\right)\right] u(\bar{r}, z) = 0 \quad (1)$$

Where

- $k^2 = \omega^2 \mu_0 \varepsilon_0 \langle \varepsilon_r \rangle = k_0^2 \langle \varepsilon_r \rangle$ is the local wave number
- μ_0, ε_0 and k_0 are the free space permeability, permittivity and wave number
- $\bar{r}$ is one observation point inside the medium and z is the coordinate along the direction of propagation.

Assuming that the variation of the complex amplitude is mainly in the direction perpendicular to the main propagation axis (parabolic approximation), it can be transformed into a Parabolic Equation (PE). he stochastic PE for the field complex amplitude can be written in the form

$$2jk\frac{\partial U(\bar{r}, z)}{\partial z} + \nabla_t^2 U(\bar{r}, z) + k^2 \varepsilon_1(\bar{r}, z) U(\bar{r}, z) = 0 \quad (2)$$

where ∇_t^2 is the transverse Laplacian.

To solve this equation, the medium is divided into series of successive layers (or screens) perpendicular to the main propagation axis, each one being characterized by local homogeneous statistical properties. The solution is then obtained by splitting the equation into 2 equations, one relating to scattering effects and the other one to propagation effects and iterating successively the scattering and propagation calculations. nThis is the basis of the Multiple Phase Screen (MPS) technique.

C. Results obtained

Inputs of the model are the transmitter and receiver locations, the time, day and year of observation, and the geophysical parameters. Based on the PRIS measurements campaign, experimental laws have been derived for the geographic and local time dependency. The spectrum is characterized by three parameters: the slope, a typical dimension of inhomogeneities and the strength. Default values are respectively set to p = 3, L_0 = 1 kilometre and $\sigma_{Ne} = 0.1 \langle N_e \rangle$. As geophysical parameters, only the average 10.7 cm solar flux number is considered. Its value is taken from the curves published by the National Oceanic and Atmospheric Administration (www.noaa.gov). The magnetic activity is ignored. It is not considered either in the NeQuick model.

For earth space links, the source point is the antenna onboard the satellite and the observation point is on the ground. Once the line of sight is determined, phase screens are set along this line and statistical parameters are associated to each one of these screens. The algorithm provides the field $U(r)$ at the observation point, where r is the dimension transverse to the direction of propagation. Dependency of the received field on the time can be obtained, considering both the source displacement and the medium drift velocity. A time series of the received field is obtained in that case.

GISM calculates a mean value of the scintillation indices both for intensity and phase fluctuations. The fluctuating medium is assumed to be statistically homogeneous. This could be improved however including a dependency of the statistical parameters on the altitude. The reality is different to some extent. The medium has a patchy structure and links meeting the geographic and time conditions may not be affected due to this patchy structure. Consequently a probability of occurrence should be given together with the mean value. This is not provided in the current version of the model. The corresponding probability shall be obtained from measurements analysis.

Two indices are defined to characterize the scintillations: the standard deviation of the normalized intensity, named S4, and the phase standard deviation. The scintillation event strength is defined with respect to the S4 value which is between 0 and 1. A value of 1 will correspond to about 35 dB peak to peak of intensity fluctuations. One example of the time series provided by the model is represented on Figure 1 for a strong fluctuation case. The scintillation indices are calculated from these 500 s. samples (intensity and phase). The scintillation strength is weak (S4 < 0.3), medium (0.3 < S4 < 0.6) or strong (S4 > 0.6) depending on the case. This usual classification refers to the fade levels and the resulting constraints on a navigation system, from -2 dB to + 2 dB in the weak regime to more than 20 dB peak to peak for the strong regime.

D. Comparisons with measurements

The results reported hereafter are taken from the PRIS measurement campaign (Béniguel, 2009) carried out under ESA / ESTEC contract N° 19530. For this study, a number of receivers were deployed both at low and high latitudes, in particular in Vietnam, Indonesia, Guiana, Cameroon, Chad and Sweden. These receivers were dedicated receivers, operating at 50 Hz. A data bank was constituted and the scintillation characteristics were derived from an extensive analysis of this data bank. Comparisons between measurements and results provided by the GISM model in the same conditions were performed both for the scintillation indices and on the spectrum.

<u>Scintillation indices</u>

One week of measurements at Cayenne, French Guiana was selected. The results are presented in the Figures 1. The x axis corresponds to local time at receiver location. The 0 value has been set arbitrarily to Saturday 19:00, the week of observation.

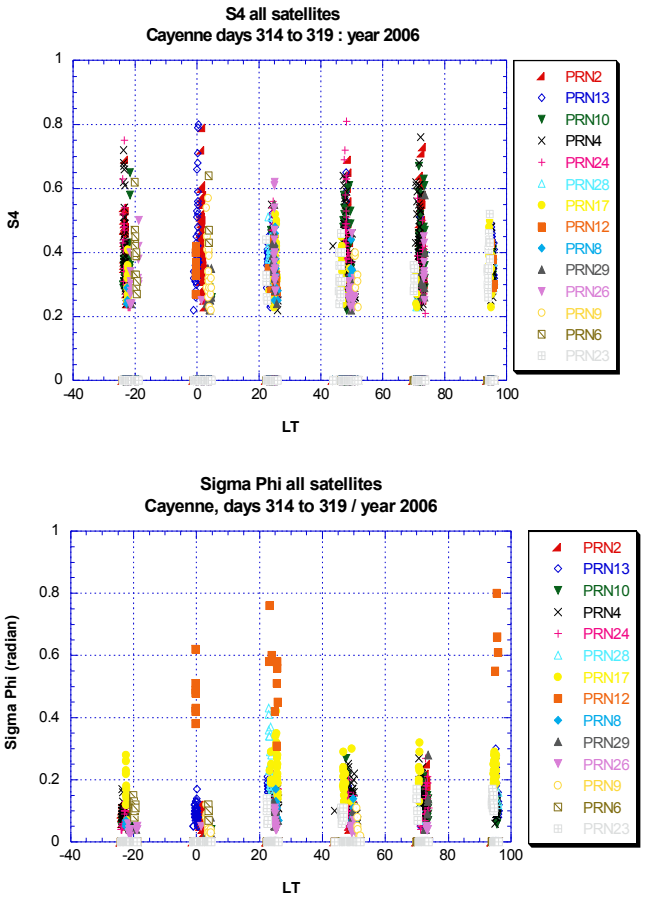

Figure 1: Intensity and phase scintillation indices measurements on GPS week N° 377

Measurements

The local time of the x axis corresponds to hours in GPS time. Each point corresponds to a 1 minute sample. Only points with a S4 value greater than 0.2 were retained in the analysis. A 5° mask elevation angle was taken when recording the data. In addition multipath is rejected using the code carrier divergence algorithm recommended in the Novatel GSV 4004 user manual. As can be seen on Figure 3, the points are clustered every evening at post sunset hours, typically 19:00 - 24:00. No average is taken on the data. The scintillation activity occurred quite regularly that week with comparable levels. The S4 average value is about 0.4. The flux number that week (GPS week N° 377, modulo 1024) was equal to 90.

The phase fluctuations are plotted concurrently. The mean value is about 0.2, consequently lower than the S4 value. This observation is quite common. A few points exhibit high values. Deep fades occur concurrently to these high values. In the case of very small values this creates phase jumps. As a consequence the phase and intensity standard deviations are no longer related.

The scintillation characteristics, both indices and spectral parameters, have been calculated using 1 minute samples. This calculation brings no particular difficulty for the intensity, which practically does not change during one minute. The calculation of the phase parameters is more difficult. A high pass 6th order filter is used to remove the low frequency components of the signal, due to the satellite motion on its trajectory.

Modelling

The scenario was replayed using the corresponding Yuma files for one particular day of the week (cf Figure 3). A different day will not bring significant differences considering that the geophysical parameters would have been quite identical. The flux number, input to GISM, has been set to 90. As mentioned previously, the model provides a mean value. It overestimates the number of affected links due to the fact that the probability of occurrence is not considered. Only the mean values can be compared. The scintillation intensity index mean value is about 0.4, corresponding to the measurements. The scintillation phase index mean value is slightly greater than the one recorded in the measurements. In both cases the phase RMS is lower than the intensity RMS, and in both cases some points exhibit high values due to the phase jumps.

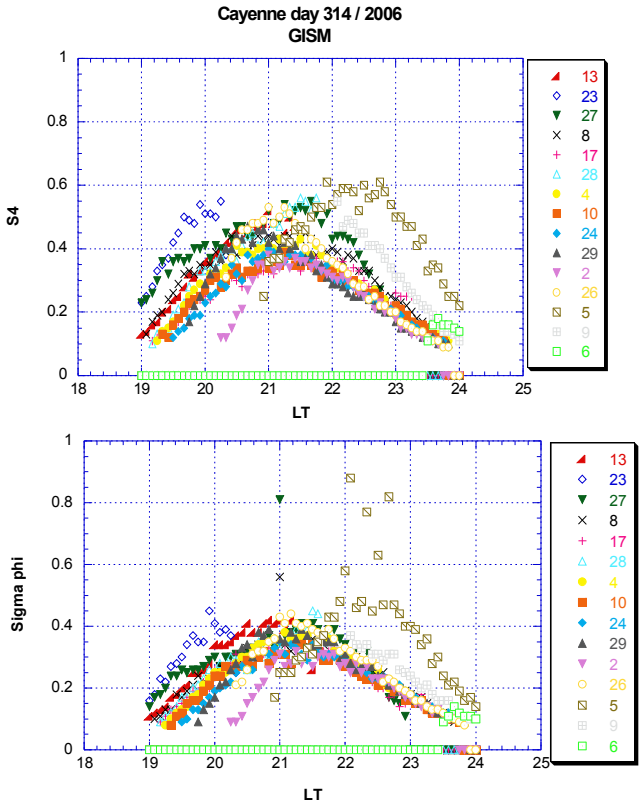

Figure 3: Intensity and Phase scintillation indices on day 314, GPS week N° 377, obtained by modeling

III. SECOND ORDER MOMENT OF THE FIELD

For a radar application, the coherence properties of the transmitted field are required. The mutual coherence function (MCF), noted Γ, characterizes the coherence properties of the transmitted field and its determination is required for a radar application.

$$\Gamma(z, k_1, k_2, r_1, r_2) = \left\langle U_1(z, k_1, r_1)\ U_2^*(z, k_2, r_2) \right\rangle \qquad (3)$$

The Γ function is obtained starting from equation (2) written for two frequencies and two positions, then combining the different equations (Ishimaru 1978). The final equation is written below:

$$\left[2j\frac{\partial}{\partial z} + \frac{1}{k_1}\nabla_{t1}^2 - \frac{1}{k_2}\nabla_{t2}^2 + \frac{j k_p^4}{4}\left[\left(\frac{1}{k_1^2}+\frac{1}{k_2^2}\right)A_\xi(0) - \frac{2}{k_1 k_2}A_\xi(\rho)\right]\right]\Gamma(z,\rho) = 0 \qquad (4)$$

Where

- $B_\varepsilon(z,\rho) = \langle \varepsilon(r_1)\ \varepsilon(r_2) \rangle$ is the autocorrelation of permittivity fluctuations
- $\xi = \sigma_{Ne} / Ne$ and Ne is the electron density
- $A_\xi(\rho) = \int B_\xi(z,\rho)\, dz$
- ∇_{t1}^2 , ∇_{t2}^2 are the Laplacians with respect to r_1 and r_2 and $\rho = r_1 - r_2$

Equation (4) can be re-organized as written below:

$$\left[\frac{\partial}{\partial z} - \frac{j}{2}\frac{k_d}{k^2}\nabla_d^2 + \frac{\lambda^2\sigma_\Phi^2}{8}\left[\frac{k_d^2}{\pi^2 L} + 2k^2\rho^2\frac{\mathrm{Log}(L_0/\ell_i)}{2\pi^2 L_0^2 L}\right]\right]\Gamma(z,\rho) = 0 \qquad (5)$$

This new expression is again a parabolic equation. It can be solved using the same technique as the one presented in section 2. It is two dimensions with respect to distance and frequency separation. In the transform domain, it provides the medium scattering function dependency with respect to Doppler frequency and delay.

The algorithm is similar to the one used for equation (2), alternating scattering and propagation calculation. In addition, if a quadratic approximation of the phase structure is used, which can be demonstrated whatever the spectrum slope value is, most of the calculations can be performed analytically, (Nickisch, 1992), (Knepp and Nickisch, 2009).

Despite the fact that the Γ function depends on two variables, the Fourier transforms reduce to a one dimension FFT, the second transformation being done analytically.

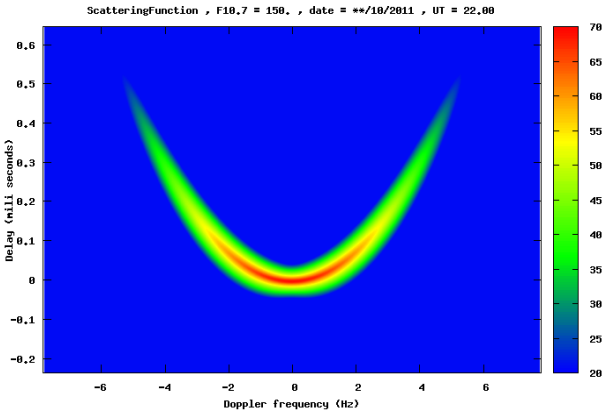

Figure 6: Mutual coherence function ; one single screen HF propagation (left panel, large Q value) and P band propagation (right panel, Q value around 1)

The result presented on Figure 6 has been obtained in HF. A spread factor, named Q, related to the medium parameters can be defined and depending on its value, the shape of the scattering function may change significantly. The inhomogeneities sizes, the frequency and the distances have a strong influence on the signal spreading.

In the case of one single screen the whole calculation can be performed analytically. The solution is given by the expression below where S, B and P are functions of the phase variance, the frequency and the medium parameters as introduced by (Nickisch, 1992)

$$\Gamma(\tau, K_x, z) = \frac{z}{2\sqrt{SB}}\exp\left(-\frac{z^2K_x^2}{4S}\right)\exp\left(-\frac{(\tau + z^2K_x^2P)^2}{4B}\right) \qquad (7)$$

with $$B = \frac{\sigma_\Phi^2}{2\omega^2}\ ;\ S = \sigma_\Phi^2 L^2 \frac{\mathrm{Log}(L_0/\ell_i)}{6\pi^2 L_0^2} \qquad (8)$$

and $$P = \frac{1}{2 c k^2}\left(\frac{1}{z_{i+1}} - \frac{1}{z_i}\right) \qquad (9)$$

z_i is the coordinate along the propagation direction.

This expression allows conducting a parametric analysis study.

Figure 6 below shows another example. The frequency is P band and the spread factor is different with as a consequence a different shape than previously. In addition we have considered the case of a SAR antenna and the antenna gain for a virtual antenna of 10 km long is included.

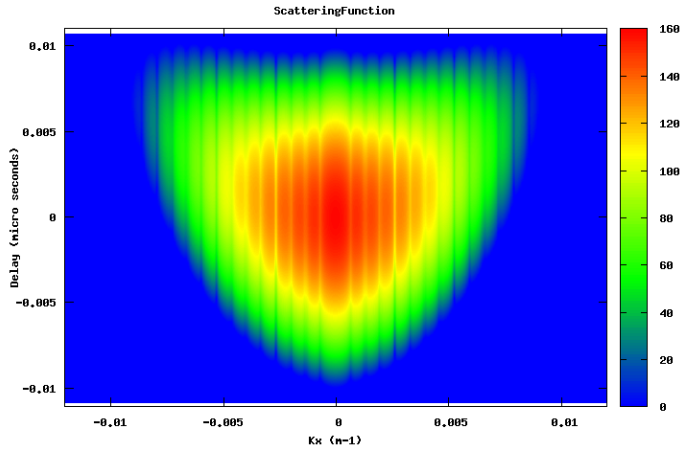

Figure 7: Mutual coherence function in P band including the antenna pattern. The Q parameter value is around 1.

IV. CONCLUSION

The GISM model, presented in this paper, uses a classical phase screen technique algorithm. Sub models have been included to estimate some specific parameters and take the geophysical dependencies into account. This concerns in particular the local time and seasonal dependency, the spectrum parameters, the inhomogeneities dimensions and their correlation distance. They were derived from measurement campaign results.

When compared to measurements, the modeling results show a relatively good agreement as presented above. Some work still needs to be done with respect to the phase characterization and to the calculation of its spectral parameters. No results were presented for high latitudes. Data from this region will be collected in the framework of the Monitor campaign. Monitor is a new ESA promising measurement campaign, currently ongoing, with a higher level of requirements (Prieto Cerdeira, 2011).

The last section is focused on the calculation of the transmitted field mutual coherence function and first application to a SAR analysis. One analytical solution has been derived by assimilating the medium to one single phase screen. Comparisons for this point were made only with respect to published results. The characterization of this function is of particular interest for radar observations and remote sensing applications.

REFERENCES

[1] Béniguel Y., P. Hamel, "A Global Ionosphere Scintillation Propagation Model for Equatorial Regions", Journal of Space Weather Space Climate, 1, (2011), doi: 10.1051/swsc/2011004

[2] Béniguel Y., J-P Adam, N. Jakowski, T. Noack, V. Wilken, J-J Valette, M. Cueto, A. Bourdillon, P. Lassudrie-Duchesne, B. Arbesser-Rastburg, Analysis of scintillation recorded during the PRIS measurement campaign, Radio Science, Vol **44**, doi:10.1029/2008RS004090, 2009

[3] Carrano C., K. Groves, The GPS segment of the AFRL-SCINDA global network and the challenges of real time TEC estimation in the equatorial ionosphere, paper presented at ION NTM, Inst. Of Navigation, Monterey, Calif., 18-20 January, 2006.

[4] Costa E., E. de Paula, L. Rezende, K. Groves, P. Roddy, E. Dao, M. Kelley, « Equatorial scintillation calculations based on coherent scatter radar and C/NOFS data, Radio Science, Vol **46**, doi :10.1029/2010RS004435, 2011

[5] Gherm V., N. Zernov, H. Strangeways, Propagation model for transionospheric fluctuating paths of propagation: simulator of the transionospheric channel, Radio Science, Vol **40**, RS1003, doi:10.1029/2004RS003097, 2005

[6] Ishimaru A., Wave propagation and scattering in random media, Vol. **2**, Academic Press, ISBN 0-12-374702-3, 1978

[7] Jayachandran P. T., R. Langley, Canadian high arctic ionospheric network (CHAIN) , Radio Sci., Vol. **44**, doi:10.1029/2008RS004046, 2009

[8] Knepp D., Multiple phase screen calculation of the temporal behavior of stochastic waves, Proceedings of the IEEE, Vol **71**, N° 6, 1983

[9] Knepp D., L. J. Nickisch, Multiple phase screen calculation of wide bandwidth propagation, Radio Science, Vol **44**, doi:10.1029/2008RS004054, 2009

[10] Nickisch, L.J. Non uniform motion and extended media effects on the mutual coherence function: An analytic solution for spatial frequency, position and time, Radio Sc. Vol **27 (1)**, 1992

[11] Prieto Cerdeira R., Y. Béniguel, "The Monitor project: architecture data and products", IES Symposium, Alexandria, Va, May 2011

[12] Radicella S.M., The NeQuick model genesis, uses and evolution, Annals of Geophysics, Vol **52 (3-4)**, 2009.

[13] Rogers N., P. Cannon, K. Groves, "Measurements and simulations of ionospheric scattering on VHF and UHF radar signals: channel scattering function", Radio Science, Vol **44**, doi:10.1029/2008RS004033, 2009

[14] Valladares C., Sensing space weather with distributed observatories and the human network, presented at the Satellite navigation science and technology for Africa workshop in Trieste, April 2009

[15] Wernik A., L. Alfonsi, M. Materassi, Scintillation modeling using in situ data, Radio Sci., Vol. **42**, doi:0.1029/2006RS003512, 2007